Reassessment of Long-Term Performance of Geogrids by Considering Mutual Interaction among Reduction Factors

Han-Yong Jeon[1] and Yuan Chun Jin[2]
Division of Nano-Systems Engineering/Inha University, Incheon, Korea (South);
Tel: +82-32 860 7492; Fax: +83-32 872 1426;
[1]*Email:* hyjeon@inha.ac.kr

ABSTRACT: For estimating allowable tensile strength of geogrids by reduction factor, it has a limit not to consider interaction force among reduction factors. Junction strength would be reduced by installation damages or chemical degradation as same as tensile strength. Single junction test method cannot properly cover for damaged samples and shows large deviations as it does not consider scale effect. Especially for calculating shear strength, no reasonable study to consider all reduction factors was conducted yet. Therefore, in this study, (a) reduction factors that may affect the long-term performance of geogrids were revaluated to consider various application conditions and (b) accurate long-term allowable tensile strength was calculated to consider interrelation among reduction factors. Creep results after installation damage and chemical resistance test showed lower value than that of GRI GG-4 calculation. After installation damage and chemical resistance test, the reduction factor of junction strength was less than that of tensile strength. Finally, shear strength before and after installation damage showed no change before and after installation.

KEYWORDS; reduction factor, junction strength, scale effect, long-term performance, GRI GG-4

1. INTRODUCTION

Most geosynthetic-reinforced soil structures have longevity designed to last up to 100 years (Koerner, 2005). This implies that the corresponding reinforcement will last accordingly. The properties of a geosynthetic generally depend on time. The current design approach to account for installation damage and long-term degradation is to divide the ultimate tensile strength by particular reduction factors (Koerner, 2005, Hufenus et al, 2005, Shuka et al, 2002). Allen and Bathurst (2002) demonstrate through back-analysis of available wall case histories, that geosynthetic reinforcement load levels appear to be significantly lower than values estimated using the North American design methods.

The cause of conventional design results from consideration of a safety factor in terms of civil engineering and uncertainty of short-term and long-term properties of materials. Uncertainty of material comes from combination of each factor that may change the total reduction factor.

So, if total reduction factor is calculated considering combination of each factor, it would certainly reduce uncertainty and thus save cost (Hsuan and Yeo, 2005, Koo, H.J. and Kim, 2005, Tatsuoka and Kongkitkul, 2007). Looking at the study of Allen and Bathurst (1996), the long-term behaviour of damaged geogrids upon construction showed the decreasing result based on isochronous curve.

On the other hand, Billing. et al (1990) studied creep behavior of PP woven textile, geostrip and HDPE geogrid after installation damage; and in case of PP woven geotextile, they reported that it showed relatively a little creep strain compared to a specimen before damage.

Besides, in case of geostrip, it was reported that it almost never showed installation damage by PP coating which is a characteristic of the product. Cho. et al (2006) evaluated installation damage at maximum particle 40, 60, 80mm, and then among them, assessed creep characteristics of some specimens. As the size of filling material is larger, reduction factor of installation damage was represented to be larger.

However, the studies on creep characteristics according to maximum particle size have not been conducted. Up to now, the creep test by damaged specimens upon construction focused on only the variety of geosynthetics material or construction conditions and the studies on variation of reduction factor by characteristics of soil have never been implemented.

Besides, the studies on the effect of chemical degradation on creep characteristics have not been conducted either. In previous research, when coating material was destructed, it could be known that chemical degradation occurred under the condition of pH=9. In this study, creep characteristics by damage upon construction due to two types of filling materials were evaluated and the effect of installation damage and chemical degradation on creep characteristics was comprehensively reviewed and then its value was compared with GRI GG-4 test value [11].

Decrease of the allowable junction strength depends on short-term effects like installation damage, which reduce the maximum junction strength but do not further affect the long-term properties and on effects like creep and aging by hydrolysis, oxidation and/or abrasion, which result in long-term junction strength loss. The reduction factor of junction strength is different from tensile strength due to the difference in physical and chemical structure. Therefore, correct junction strength reduction factor is the key point to calculate allowable junction strength. Hsieh. et. al. (2000) evaluated junction strength of PET geogrids after installation damage using GRI GG-2 test method [13]. Installation damage test uncertainty is large and damage on each specimen will be different. But, GRI GG 2 test method does not consider scale effect that creates large deviation in the test results as well as lowers the accuracy.

To evaluate the tensile strength of damaged geogrid, wide-width tensile strength test method is used. Hence, multi junction test method is more appropriate to evaluate junction strength of damaged geogrid considering the scale effect and thus uncertainty of results can be reduced (Jeon and Yuu, 2003, Jeon and Jin, 2011). Moreover, effect of chemical degradation on junction was not researched before. Here, in this experiment, effect of installation and chemical degradation on junction strength was evaluated using multi-junction clamp. Both individual effect and combined effect of the factors were observed.

By the way, in the case of installation of geogrids on site, the design model regarding the strength reduction according to the installation damages was suggested but any definite model for the change of shear behavior according to the occurring changes upon installation was not suggested. Especially, since the shear property is an important factor that determines the long-term performance of civil structures in case of the slope reinforcement, the design model that predicted the change of performance considering the damages by compacting work and equipment upon construction must be suggested.

Therefore, considering the damage of geogrids that inevitably occurs upon construction on site, a proper model for the construction conditions on site must be applied. This study looked at the change of shear behavior by the damage of geogrids before and after installation damage, and theoretically analyzed the shear behavior by the installation damage.

2. EXPERIMENT

2.1 Materials

For the samples to be used for this experiment, three kinds of geogrids were used such as woven type(WG), warp knitted type(WKG) and welded type(WBG), and the design strength was 6Tons, 8Tons and 10Tons(6T, 8T and 10T) respectively. The yarn of all geogrids is polyethylene terephthalate (PET) and the coating material of woven geogrid and warp knitted geogrid is polyvinyl chloride (PVC). But the coating material of welded geogrid is polypropylene (PP). And the specification and physical properties of geogrids were represented in Table 1.

Table 1 Specifications of geogrids

Geogrid	Raw Material/ Coating polymer	Number of ribs (/m)	Mechanical properties	
			Ultimate tensile strength (ton/m)	Elongation at Break (%)
WG-8	PET/PVC	42	10.1	10.7
WKG-8	PET/PVC	38	10.8	11.9
WBG-6	PET/PP	25	7.9	11.1
WBG-8	PET/PP	25	10.8	11.9

2.2 Reduction factor test

To obtain reduction factor RF, the samples were evaluated with ①installation damage (RF_{ID}), ②chemical resistance (RF_D) and ③creep test (RF_{CR}). Combination effects between each RF were obtained by subsequent RF test. For example, Combination effect between RF_{ID} and RF_{CR} was obtained by creep test after installation damage test. Filling materials (soil) and 4.75-37.5 mm particles (gravel) were used to test installation damage individually. The experiment was conducted in accordance to ENV ISO 10722-1 and load cycle was taken 200. Tensile and junction properties of geogird were tested according to ASTM D4595 [16, 17].

Original and installation damaged geogrids were immersed in closed beakers in NaOH (pH=9, pH=13) buffer solutions. Then, beakers were placed in temperature-controlled ovens. A sample was collected at each month, the single rib tensile strength was measured, and the chemical resistance was evaluated.

Creep tests were performed on the original geogrids, installation damaged geogrids and installation damaged with the chemical treated geogrids. Accelerated creep tests were performed on woven geogrids using the accelerated creep test equipment. The load level of 50-78% ultimate tensile strength was applied to woven geogrids. Each specimen was allowed to reach equilibrium at 20℃ prior to test initiation. Temperature was stepped 14℃ every 10000 seconds starting 20℃ and ending to 76℃. Creep strains for the geogrids are plotted versus log time at each level of temperatures.

2.3 Junction strength test

Junction strength of original geogrids, installation damaged geogrids and installation damaged with the chemical treated geogrids were tested using multi-junction clamp according to ASTM D4595.

2.4 Direct shear test

The filling material that was used for the direct shear test was soil from the real construction site, and Figure 1 shows grain size distribution of the filling material. The soil used for the filling material is classified into SW (Sand Wedge) by unified soil classification system, and the direct shear strength was measured at each interface by using the medium-scaled direct shear test device (Figure 2) on the basis of ASTM D5321 [18].

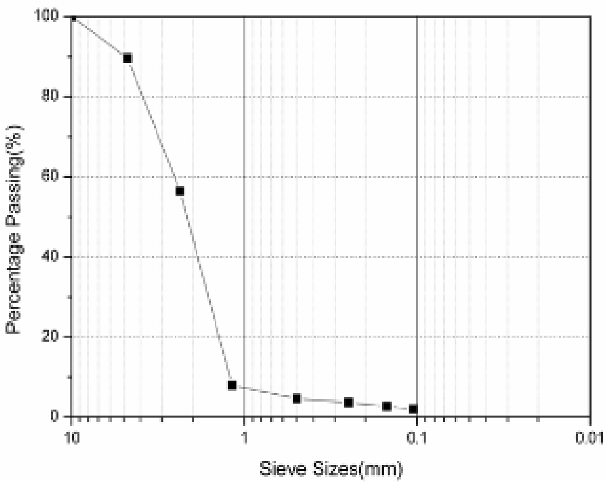

Figure 1 Grain size distribution of test soils

(a)Mid-scale direct shear test apparatus

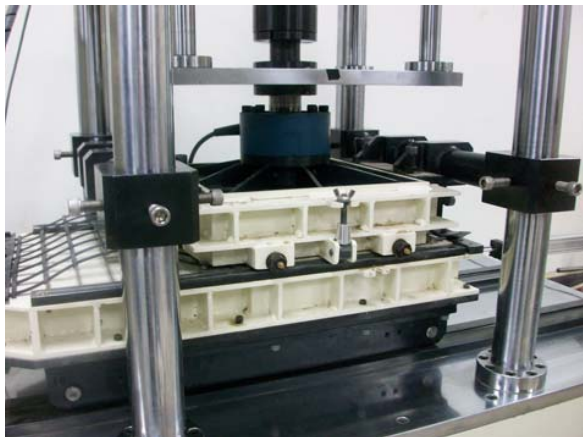

(b)Side view of shear interface in testing process

Figure 2 Photographs of mid-scale direct shear test apparatus

3. RESULTS AND DISCUSSION

3.1 Combination effect between RF_{CR}, RF_{ID}, RF_D

Figure 3 and 4 show the percentage of tensile strength retention of WG-8 after different chemical exposure. There was merely small amount of decease in original and specimen of installation damage in soil (IDS) after exposure to pH=9. In contrast, there was decrease in specimen of installation damage in gravel (IDG) at pH=9. This is cause of PVC coating material destroyed during installation test and PET filament directly exposed to solutions and got the chemical degradation. It may be a problem if continuously chemical degradation occurs on geogrids as it is expected that service life of geogrid's is 50-100years. Since WG-8 showed less than 10% decrease in extreme condition (pH=9, 50℃, and installed in gravel), it can be predicted that in real environment chemical degradation followed by installation damage is very limited. Moreover, it hardly reaches to the activation energy for chemical degradation as temperature in reinforcement wall is usually lower than 20℃. But in some specific conditions, like slope of landfills, the temperature may over 50℃. It may require caution to use geogrids at high alkali condition and more time is needed to evaluate chemical degradation properly. The tensile strength decreased much in severe alkaline condition pH=13. Especially IDG showed tensile strength retention of 64.4%.

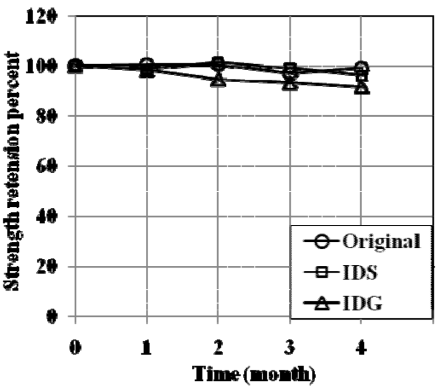

Figure 3 Rib tensile strength retention percent of WG-8 with exposure conditions (pH=9, 50℃)

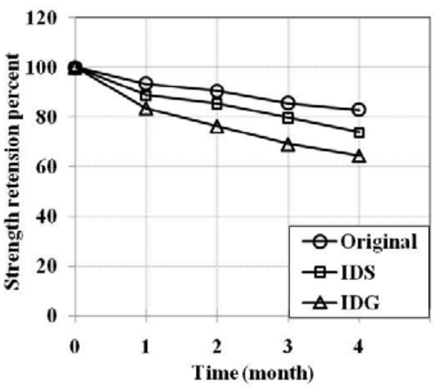

Figure 4.Rib tensile strength retention percent of WG-8 with exposure conditions (pH=13, 50℃)

Under the condition of pH=9, 50℃, creep characteristic of WG-8 that was exposed for 4 months was represented (Figure 5, Table 2). In case of 50% and 60% of UTS, they shows the stable behavior during test period, there was not a rupture in the case of 65%, but it showed strain exceeding 7.5% that is a limited strain. There was creep rupture in case of 68% and 75%. After chemical exposure, it showed almost similar strain under the same load. Therefore, it could be known that there was little change of creep characteristic after chemical exposure.

Figures 6-7 and Table 3-4 show the resulting creep properties of the WG-8 after installation damage. After installation damage, the value of creep strain is higher than that of without installation damage at the same load. This is because some of the filaments are greatly damaged or torn by the installation damage that the remaining filaments suffered higher load than usual. In case of IDS, it showed stable behavior during test period in case of 50% and 60% of UTS, and there was creep rupture under the load more than 65%. On the other hand, in case of IDG, it showed stable behavior only at 50% of UTS and there was creep rupture under the load more than 60%.

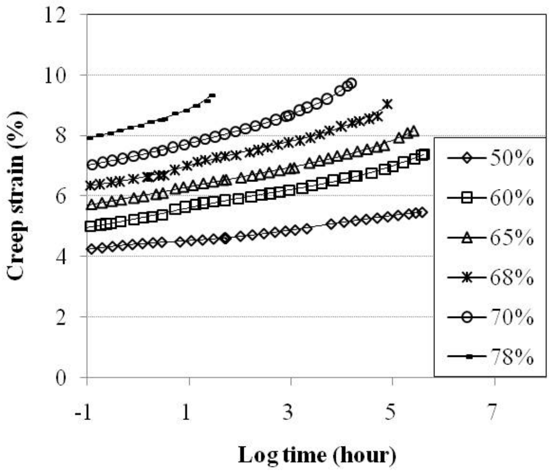

(a)

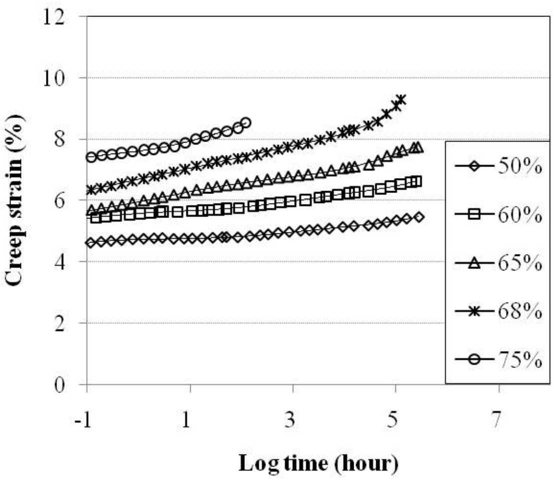

(b)

Figure 5 Tensile creep master curve of WG-8 (a)original (b)after chemical exposure (pH=9, 50℃ ,4 months)

Table 2 Results of creep test after chemical exposure (pH=9, 50℃, 4 months)

Specification	Applied stress(% of UTS)				
	50	60	65	68	75
Log time (hour)	5.45	5.30	5.35	5.10	2.09
Elongation (%)	5.49	6.60	7.72	9.30	8.55
Condition	Continue	Continue	Continue	Rupture	Rupture

Figures 8-9 and Table 5-6 show the resulting creep properties of the WG-8 after installation damage and chemical degradation. The experiment result turned out to be similar with the case considering only installation damage. In case of IDS, it showed stable behavior during test period in case of 50% and 60% of UTS and there was creep rupture under a load more than 65%. On the other hand, in

Table 3 Results of creep test after installation damage (soil)

Specification	Applied stress (% of UTS)				
	50	60	65	68	75
Log time (hour)	5.45	5.79	4.98	2.21	1.62
Elongation (%)	6.32	7.99	8.98	8.95	8.73
Condition	Continue	Continue	Continue	Rupture	Rupture

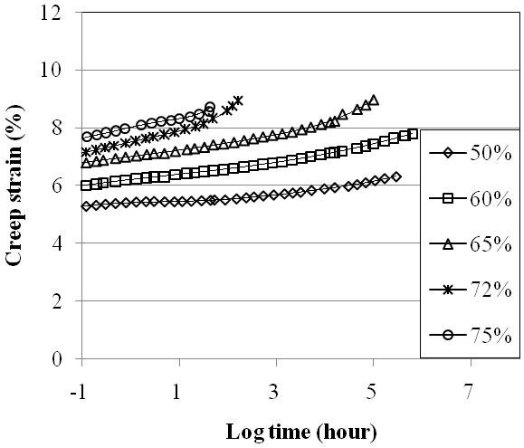

Figure 6 Tensile creep master curve of WG-8 after installation damage (soil)

Table 4 Results of creep test after installation damage (gravel)

Specification	Applied stress (% of UTS)			
	50	60	65	68
Log time (hour)	5.49	4.65	4.12	1.15
Elongation (%)	7.46	8.83	9.6	8.97
Condition	Continue	Rupture	Rupture	Rupture

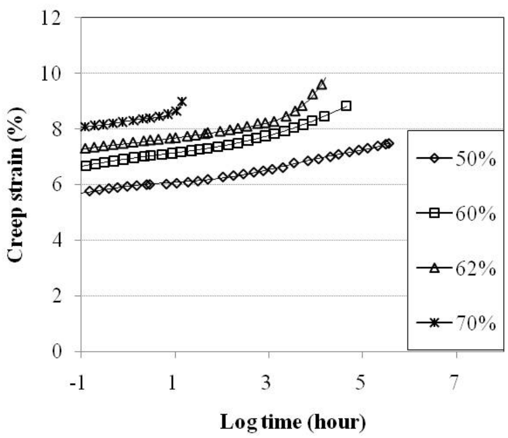

Figure 7 Tensile creep master curve of WG-8 after installation damage (gravel)

Table 5 Results of creep test after installation damage and chemical exposure (pH=9, 50℃, soil)

Specification	Applied stress (% of UTS)				
	50	60	65	68	70
Log time (hour)	5.40	5.39	5.01	4.09	3.21
Elongation (%)	6.22	8.15	9.67	9.82	10.27
Condition	Continue	Continue	Rupture	Rupture	Rupture

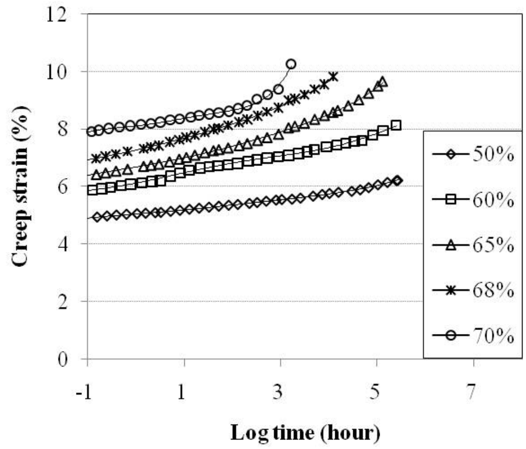

Figure 8 Tensile creep master curve of WG-8 after installation damage and chemical exposure (pH=9, 50℃, soil)

Table 6 Results of creep test after installation damage and chemical exposure (pH=9, 50℃, gravel)

Specification	Applied stress (% of UTS)			
	50	60	65	68
Log time (hour)	5.71	4.87	3.14	1.09
Elongation (%)	8.07	10.09	8.98	8.30
Condition	Continue	Rupture	Rupture	Rupture

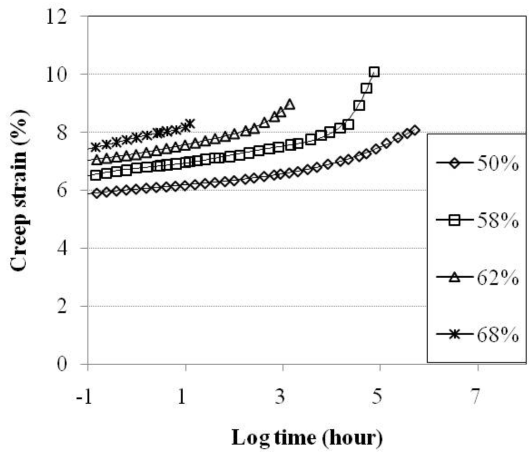

Figure 9 Tensile creep master curve of WG-8 after installation damage and chemical exposure (pH=9, 50℃, gravel)

case of IDG, it showed stable behavior under only 50% of UTS and there was creep rupture at 58% of UTS as well. From this, it can be known that the effect of chemical exposure condition (4 months, 50℃) on creep characteristic was limited.

Figures 10-13 show isochronous curve at each condition, and Figures 14 and 15 show each regression analysis diagram, and the calculated reduction factors were represented in Table 7. GRI GG-4 is a conservative test method, includes sufficient reduction factors to be considered to predict long-term properties of geogrids.

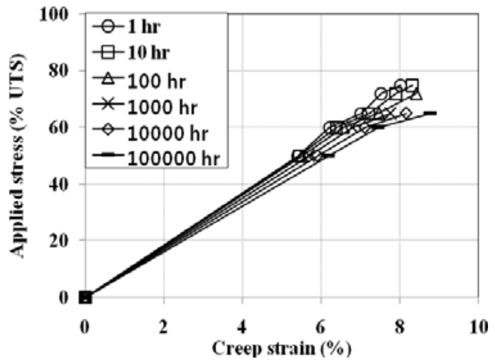

Figure 10 Isochronous curve of WBG-6 after installation damage in soil

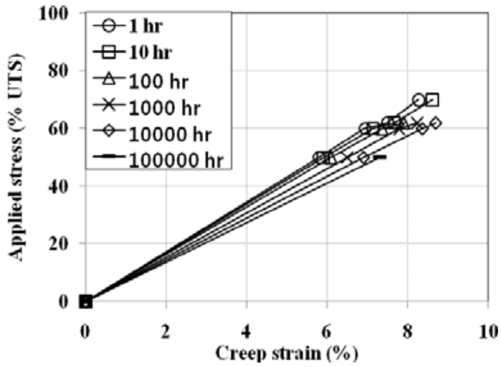

Figure 11 Isochronous curve of WBG-6 after installation damage in gravel

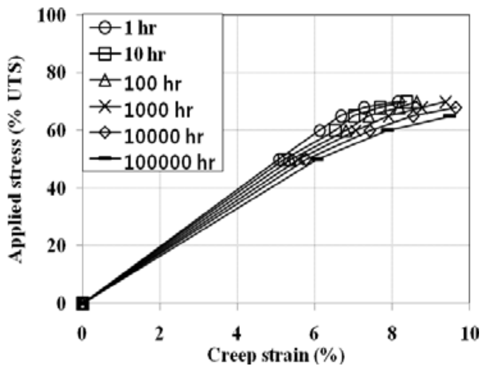

Figure 12 Isochronous curve of WBG-6 after installation damage in soil and chemical exposure

The resulting reduction factor is formulated in a traditional matter,

$$RF_{ID}=T_{ult}/T_{exh} \qquad (1)$$

where, RF_{ID}=reduction factor for installation damage; T_{ult}= ultimate tensile strength form standardized in isolation tensile test; T_{exh}=exhumed strength of the geogrids in ASTM D4595, GRI GG-1 or GRI GG-2.

The factor of safety is obtained as follows:

$$RF_{CD}=1/1-[R_{50\text{-}120}] \qquad (2)$$

where, RF_{CD}=reduction factor for chemical degradation; $R_{50\text{-}120}$=strength reduction ratio of the 50℃ incubation test at 120 days exposure (absolute value).

The creep reduction factor is determined by GRI GG-4 as expressed in Equation 3:

$$RF_{CR} = T_{ST}/T_{LT} \qquad (3)$$

where, RF_{CR} = reduction factor of creep, T_{LT} = 10^5 or 10^6 hour-design life strength of the geosynthetics, and T_{ST} = short-term strength of the geosynthetics in ASTM D4595

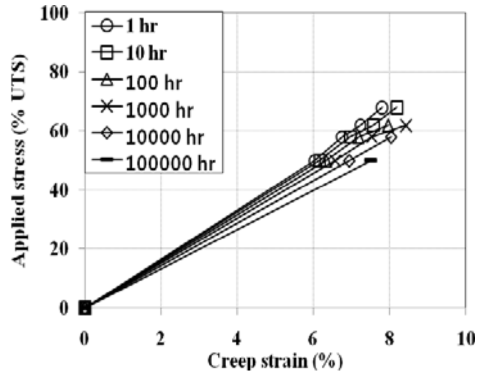

Figure 13 Isochronous curve of WBG-6 after installation damage in gravel and chemical exposure

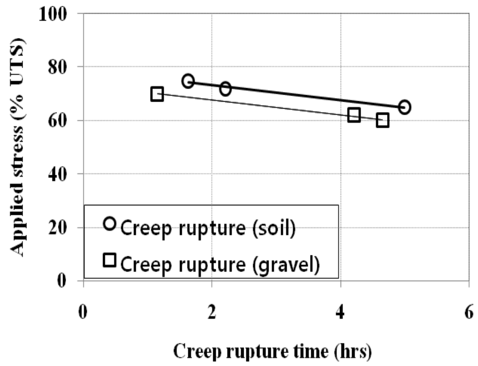

Figure 14 Plot of applied stress vs. creep rupture time of geogrid considered installation damage

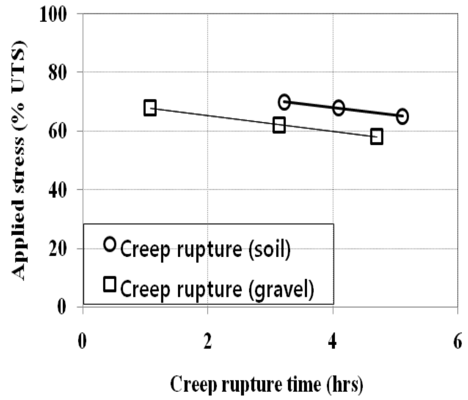

Figure 15 Plot of applied stress vs. creep rupture time of geogrid considered installation damage and chemical degradation

Table 7 Reduction factor of geogrids at pH=9, prediction after 10^6 hours (soil)

(a) soil

Reduction factor	Calculated	Tested
RF_D, RF_{CR}	1.54	1.55
RF_{ID}, RF_D	1.1	1.1
RF_{ID}, RF_{CR}	1.69	1.61
RF_{ID}, RF_{CR}, RF_D	1.69	1.59

(b) gravel

Reduction factor	Calculated	Tested
RF_D, RF_{CR}	1.54	1.55
RF_{ID}, RF_D	1.28	1.35
RF_{ID}, RF_{CR}	1.97	1.76
RF_{ID}, RF_{CR}, RF_D	1.97	1.84

There was no change in reduction factors i.e. combination of RFD and RFCR, this is cause of good chemical resistance in pH=9. Also, there was no change in combination of RFID (soil) and RFD. But tested value is higher than calculated value in the combination of RFID (gravel) and RFD. This is cause of gravel destroyed surface of coating materials and accelerated chemical degradation. However, the difference is not too much. The tested reduction factor is lower than the calculated value in the combination of RFID and RFCR, especially at gravel, lower than 12%. This is cause of mutual effect of installation damage and creep test. The same is applicable for the total reduction factor.

3.2 Interpretation of the geogrids junction Strength by installation damage and chemical degradation

A summary of the results of the tensile strength and junction strength before and after installation damage in gravel are presented in Table 8. After installation damage, the tensile strength of geogrids was significantly reduced. Especially, the tensile retention % of WKG-8 from cross-machine direction (CMD) showed 67.7. This tells that since the transverse rib of WKG-8 is weak, more damage can be caused by installation damage. In contrast the tensile retention % of WG-8 from CMD showed large value compared to machine direction (MD). This is cause of transverse rib of WG-8 has thick bundle diameter and coating. In case of junction strength, the retention % of WG-8 and WKG-8 showed relatively large values of 100 and 89% respectively. This is cause of the junction failure mechanism of woven geogrid is pulled out. So, the tensile reduction in transverse rib does not affect on the junction damage. In contrast, junction failure mechanism of warp knitted geogrid is caused of the self-rupture of cross rib. Therefore tensile strength of transverse rib and bending force are mainly determined by junction strength.

Figure 16 shows the percentage of junction strength retention of original geogrid and IDG geogrid after different chemical exposure. In case of junction strength of WG-8, there was less than 5% decrease in original and IDG geogrid at pH=9. In contrast, the percentage of junction strength retention of original and IDG geogrid showed 91.8 and 86.2 respectively in severe alkaline condition pH=13. But the value is greater than the percentage of tensile strength retention in same condition. This is cause of retention percentage of junction strength retention rely on pull out mechanism between longitudinal and transverse rib in woven geogrid. In case of junction strength of WKG-8, there was no change in original and IDG geogrid after exposure to pH=9.

Table 8 Tensile and junction strength before and after installation

Property		WG-8	WKG-8
Tensile strength-MD (KN/m)	Original	102.3	105.2
	Damaged	79.9	84.2
Retention(%)		78.1	80
Tensile strength-CMD (KN/m)	Original	33.4	37.4
	Damaged	30.8	25.3
Retention(%)		92.2	67.7
Junction strength (KN/m)	Original	5.5	12.3
	Damaged	5.5	11
Retention(%)		100	89

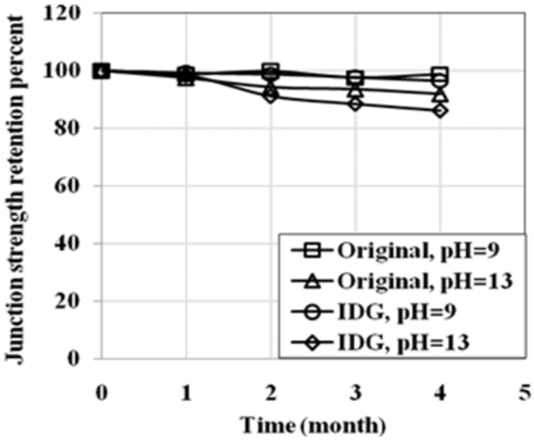

(a) WG-8

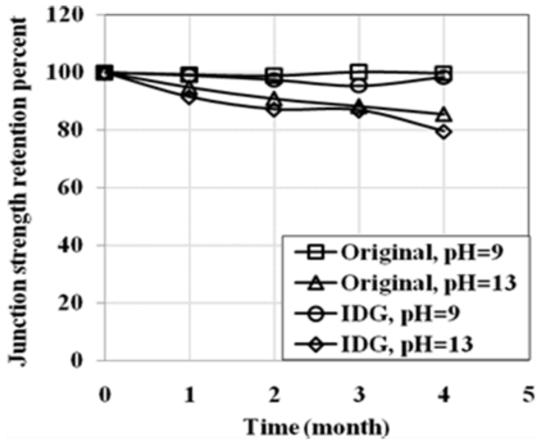

(b) WKG-8

Figure 16 Junction strength retention percent with exposure conditions

In contrast, the junction strength of original and IDG geogrid decreased much in severe alkaline condition pH=13. The difference of percentage of junction strength retention between original and IDG geogrid is very small. It showed that installation damage effect to chemical resistance of junction strength is limited.

Table 9 shows the reduction factors calculated from the retained tensile and junction strength after installation damage and chemical exposure. For both of woven and warp knitted geogrid, reduction factor in junction strength test showed lower value than that in tensile strength test. Especially in woven geogrid the value of junction strength reduction factor is negligible because of pull-out mechanism.

3.3 Interpretation of shear behavior of geogrids through index installation damage testing

3.3.1 Shear behavor before and after installation damage test

Figures 17 and 18 show the graph of shear behavior of original geogrids. According to the results of all tests, the peak strength was indicated at shearing displacement within 30mm but there was more or less difference in the behavior of post-peak strength. The post-peak strength of two geogrids at normal stress of 50,100 kPa relatively remains to be constant after reduction but it represented a phenomenon that the post-peak strength of two geogrids at normal stress of 150 kPa continuously reduced and it showed the behavior that the peak strength increased as normal stress increased. Figures 19 and 20 show the graph of shear behavior after installation damage test. After installation damage test, the shear behavior of geogrids was different from the one before the test. Compared to the status before installation damage test, there was no obvious peak strength at a specimen after installation damage test. According to the results of all tests, the shear strength showed rapidly increasing behavior up to the shear displacement within 20 mm and subsequently, it showed continuously and steadily increasing behavior.

Table 9 Junction strength reduction factor of installation damage combination with chemical degradation

Reduction factor	WG-8	WKG-8
RF_{ID}, RF_{CD}	1.35	1.29
JRF_{ID}, JRF_{CD}	1.03	1.18

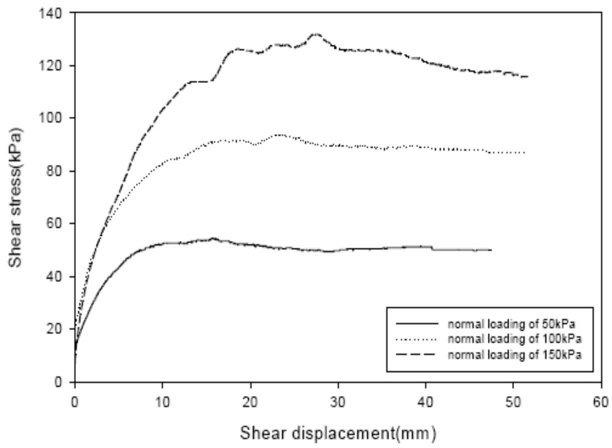

Figure 17 Stress-strain behavior of soil/WBG-6 interfaces under different loadings

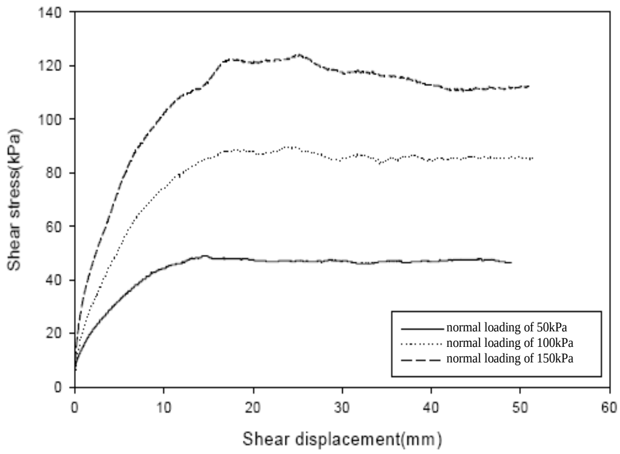

Figure 18 Stress-strain behavior of soil/WBG-8 interfaces under different loadings

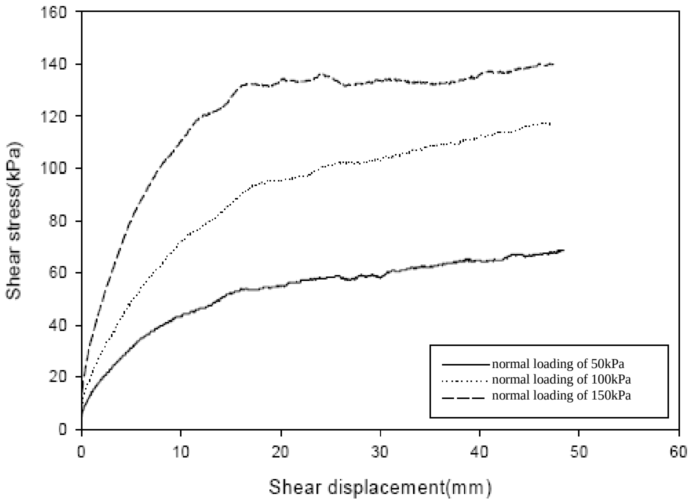

Figure 19 Stress-strain behavior of soil/installed WBG-6 interfaces under different loadings

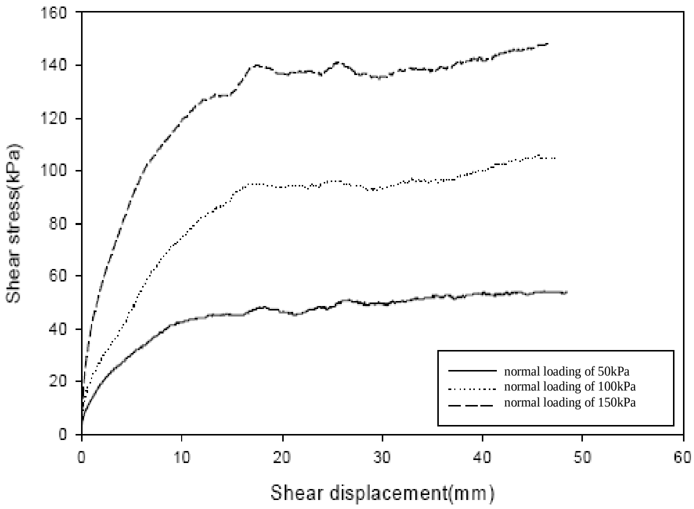

Figure 20 Stress-strain behavior of soil/installed WBG-8 interfaces under different loadings

Tables 9 and 10 show the shear stress according to normal stress before and after installation damage test. It was found that the shear strength was not relevant to the design strength of geogrids through direct shear test results. It was known that the peak value after installation damage test was almost similar to the one before installation damage test. This is thought to cause by the fact that the area in which the interaction force among soil particles occurs increases as the interaction force among soil particles in pores that are the morphological property of geogrids works and soil particles are condensed by damages on the surface of geogrids due to installation damage test at the same time. Besides, the PVC coated geogrid surface is smooth but it can be said that larger frictional force occurred as roughness of the surface took place after installation damage test.

3.3.2 Failure envelope, frictional coefficient and friction angle

The frictional coefficient can be obtained by evaluating a slope of extrapolated straight line after getting the maximum shear stress for normal stress at each interface and extrapolating it. The actual failure envelope shows somewhat the shape of a curved line but it is broadly linearly represented at the scope of experimented normal stress. Figure 21 shows the failure envelope of maximum shear stress before and after installation damage test to evaluate each frictional coefficient. In case of WBG-6, the maximum shear stress before and after installation damage test showed a similar frictional coefficient. On the other hand, WBG-8 showed a greater frictional coefficient than one before installation damage test. Tables 11 and 12 list the frictional coefficient and friction angle values before and after installation damage test.

Table 10 Shear stress of soil WBG-6 interface under different loadings

Normal loading (kPa)	Peak stress (kPa)	
	Soil/WBG-6	Soil/Wbg-6 (I.D)
50	54.47	53.92
100	94.05	93.68
150	131.81	136.17

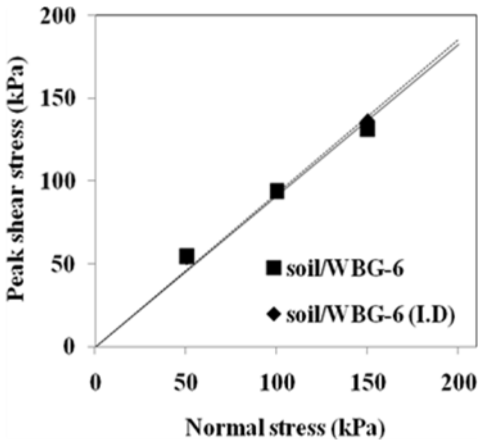

(a) soil-WB-6

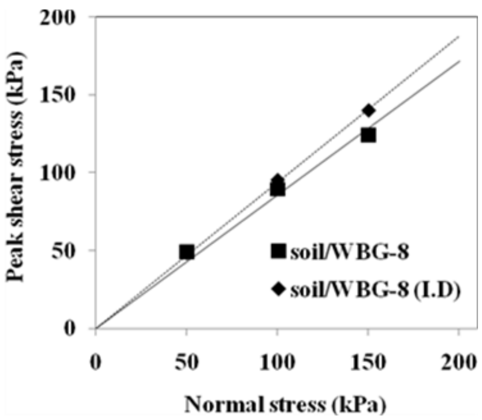

(b) soil-WB-8

Figure 21 Peak shear stress vs. normal stress plots before and after installation damage

Table 11 Shear stress of soil WBG-8 interface under different loadings

Normal loading (kPa)	Peak stress (kPa)	
	Soil/WBG-8	Soil/WBG-8 (I.D)
50	49.02	48.47
100	89.32	95.32
150	124.18	139.98

Table 12 Frictional coefficient and frictional angle of WBG-6

Geogrids	Frictional coefficient	Frictional Angle
Original	0.91	42.3
Damaged	0.93	42.9

Table 13 Frictional coefficient and frictional angle of WBG-8

Geogrids	Frictional coefficient	Frictional Angle
Original	0.86	40.7
Damaged	0.94	43.2

4. CONCLUSION

Effect of three reduction factors such as installation damage, chemical degradation and creep which affect to the long-term properties of geogrids were tested and compared. Chemical resistance decreased followed by installation damage especially at high alkali conditions showed large reduction in strength. But there was no change in pH=9 at 50℃ in soil and less than 10% of decrease showed in gravel. Creep strain showed large value after installation damage but combined reduction factor is lower than that of calculated value. Creep results after installation damage and chemical resistance test showed lower value than that of calculated value according to GRI GG-4. As a result of analyzing the shear behavior of geogrids before and after installation damage test, the post-peak strength of geogrids before installation damage test reduces after the peak strength but the post-peak strength behavior of geogrids after installation damage test showed the tendency of gradually increasing. Shear strength before and after installation damaged showed no change or increase. So, there was no change in required tensile strength. From the result of this study, it is judged that the shear behavior for damages of geogrids is similar to the case of real construction but since the strength of a specimen decreases after installation damage test, it is thought that it needs to be specified through indoor experiments simulating construction site conditions in the future. Besides, the number of compacting is limited to 200 times in the process of installation damage test in this study, which can be limited to the damage on the surface of most civil synthetic materials so it is expected that if tests and studies related to the changes of physical properties of a specimen by changing variously the number of compacting were conducted in the future, the more proper result can be obtained for site construction conditions.

5. REFERENCES

Allen, T.M. and Bathurst, R.J. (1996) "Combined allowable strength reduction factor for geosynthetic creep and installation damage", Geosynthetics International, 3, Issue 3, pp407-439.

Allen, T.M. and Bathurst, R.J., (2002) "Long–term performance of geosynthetic walls", Geosynthetics International, 9, Issue 5-6, pp575-578.

ASTM D4595. Standard Test Method for Tensile Properties of Geotextiles by the Wide Width Strip Method, ASTM International, West Conshohocken, PA.

ASTM D5321. Standard Test Method for Determining the Coefficient of Soil and Geosynthetic or Geosynthetic and Geosynthetic Friction by the Direct Shear Method, ASTM International, West Conshohocken, PA

Billing, J.W., Greenwood, J.H. and Small, G.D (1990) "Chemical mechanical durability of geotextiles", proc. of the 4th International Conference on Geotextiles, Geomembranes and Related Products, Vol.2, 621-626.

Cho, S.D., Lee, K.W., Cazzuffi, Daniele A. and Jeon, H.Y. (2006) "Evaluation of combination effects of installation damage and creep behavior on long-term design strength of geogrids, Polymer testing", 25, Issue 6, pp819-828.

GRI standard – GG4. Standard Practice for Determination of the Long-Term Design Strength of (a) Stiff and (b) Flexible Geogrids.

GRI standard-GG2. Geogrid Junction strength, Geosynthetic Research Institute, Folsom, PA.

Hufenus, R., Ruegger, R., Flum, D. and Sterba, I.J. (2005) "Strength reduction factors due to installation damage of reinforcing geosynthetics", Geotextiles and Geomembranes 23, Issue 5, pp401-424.

Hsieh, C., Wu, J.H., Lin, C.K. and Hsieh, M. (2000) "The study of the installation damage of flexible geogrids". 2nd European Geosynthetics Conference, Bologna, pp889-893.

Hsuan, Y.G. and Yeo, S.S. (2005) "Comparing the creep behavior of high density polyethylene geogrids using two acceleration methods", Geotechnical special publication, Geo-Frontier 2005, Austin, pp2887-2901.

ISO 10722-1. Geotextiles and geotextile-related products-Procedure for simulating damage during installation.

Jeon, H.Y., Yuu, J.J. Yoo, H.K. and Kim, S.H. (2003) "Assessment of junction strength of geogrids by a multi-junction test method", polymer testing 22, Issue 3, pp267-274.

Jeon, H.Y. and Jin, Y.C. (2011) "Interpretation of the junction properties of textile geogrids using multi-junction clamp", International symposium on sustainable application of geosynthetics technology, Seoul, pp87-93.

Koerner, R.M. (2005) Designing with Geosynthetics, 5th edition, Person Education Inc., New Jersey, USA

Koo, H.J. and Kim, Y.K. (2005) "Life time prediction of geogrids for reinforcement of embankments and slopes", Polymer testing 24, Issue 2, pp181-188.

Shuka, S.K. (2002). Geosynthetics and their applications, Thomas telford publishing, 210-212.

Tatsuoka, F. and Kongkitkul, W. (2007) "A theoretical framework to analyse the behavior of polymer geosynthetic reinforcement in temperature-accelerated creep tests", Geosynthetics International, 14, Issue 1, pp23-38.